Application of Weight Function Technique for Stress Intensity Factor and Failure Assessment Diagram with a Realistic Stress Profile

Kwang-Il Ho*

(*Received October 9, 1995*)

An engineering approach to calculate the stress intensity factors of a semi-elliptical crack is presented. A 2-dimensional solution is derived through weight function, by reflecting on the physical character of cracks. Flaw assessments were performed by the application of DPFAD approach with the K_I calculation for the realistic stress profile through weight function technique. The assessment points in DPFAD curve resulted in the increased safety margins. These results show the sufficient conservatism in the application of DPFAD with the weight function technique for flaw assessments, when ductile failure is expected.

Key Words: Weight Function, Stress Intensity Factor, Failure Assessment Diagram, Crack, Fracture Mechanics

1. Introduction

When assessing the structural integrity of power plant components, it is required to employ the failure assessment approach which is recommended in ASME Sec. XI. The background of ASME flaw analysis is the LEFM which is mainly applicable to the fracture phenomena of brittle material. In LEFM instability conditions were decided by Applied Stress Intensity Factor, K, and Critical Stress Intensity Factor, K_{IC} or K_{ID}, which were affected by crack length and applied stress. But pressure vessels of power plant have been operating above the transition temperature. Owing to the too much conservatism of LEFM, recently EPFM (Elastic Plastic Fracture Mechanics) approach is the new trend for the calculation of realistic safety factor. Depending on whether a brittle or ductile fracture behavior is expected under service conditions, stress intensity factor or J-integral is most widely used for failure assessments.

A representative engineering method for the EPFM is the DPFAD (Deformation Plasticity Failure Assessment Diagram)(Harison, et. al., 1976; Bloom, et. al., 1982), which was developed by EPRI and Babcock & Wilcox, based on the CEGB R-6 failure assessment diagram (Bloom, 1983). Bloom (1985) described the application for the longitudinal continuous flaw and semi-elliptical flaw which was classified as the ASME Sec. III, Appendix G-type (1989).

In this work, the mode I analysis problem of a semi-elliptical crack is treated and the stress intensity factors are calculated by using weight function and this values are applied to the Failure Assessment Diagram to show the more realistic analysis and good safety margin.

2. Analytical Study

2.1 Theoretical approach

2.1.1 Stress intensity factor through weight function

Labben et. al. (1976) introduced weight functions to calculate stress intensity factor. Bueckner (1970) and Rice (1972) demonstrated that particular function is a property of a cracked geometry.

* Department of Mechanical Engineering, The University of Suwon, Suwon, Korea

The weight function may be employed in the derivation of stress intensity factor solutions.

The weight function proposed by Bueckner (1970) for the geometry as shown in Fig. 1 is:

$$M(x, a)=\left(\frac{1}{2\pi(a-x)}\right)^{\frac{1}{2}}\cdot \left[1+m_1\left(\frac{a-x}{a}\right)+m_2\left(\frac{a-x}{a}\right)^2\right] \quad (1)$$

where m_1 and m_2 are functions of the ratio of crack depth to strip width (a/w). These values are given as:

$$m_1=N_1+O_1\left(\frac{a}{w}\right)^2+P_1\left(\frac{a}{w}\right)^6$$

$$m_2=N_2+O_2\left(\frac{a}{w}\right)^2+P_2\left(\frac{a}{w}\right)^6$$

where

$$N_1=0.6147,\quad N_2=0.2502$$
$$O_1=17.1844,\quad O_2=3.2899$$
$$P_1=8.7822,\quad P_2=70.0444$$

Then, $K_I(a)$ could be obtained from the following equation. That is,

$$K_I(a)=\int_0^a \sigma(x)M(x, a)dx \quad (2)$$

where $\sigma(x)$ is the distributed stress in the uncracked structures.

In order to obtain the exact solution for the semi-elliptical crack (Fig. 2), 3-dimensional analysis is required. But, simplification could be performed through Eq. (2) with some geometrical

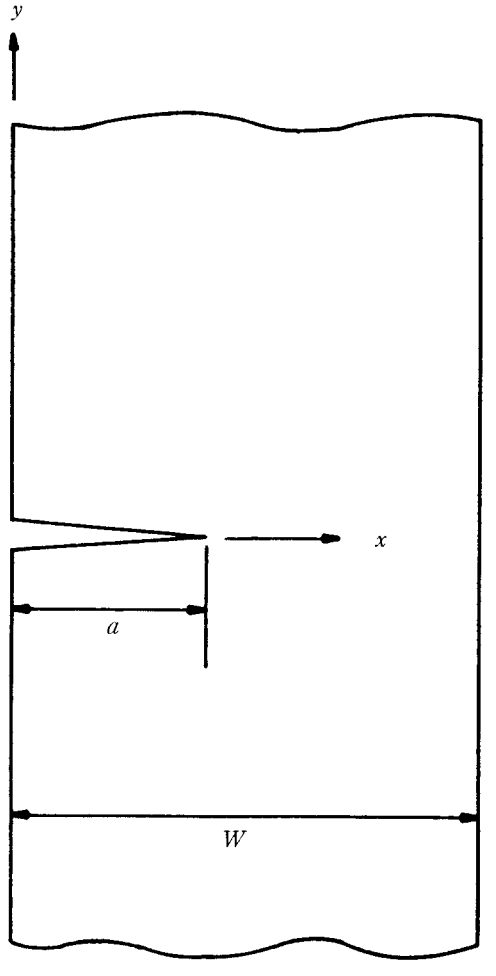

Fig. 1 Continous surface crack in an infinite strip

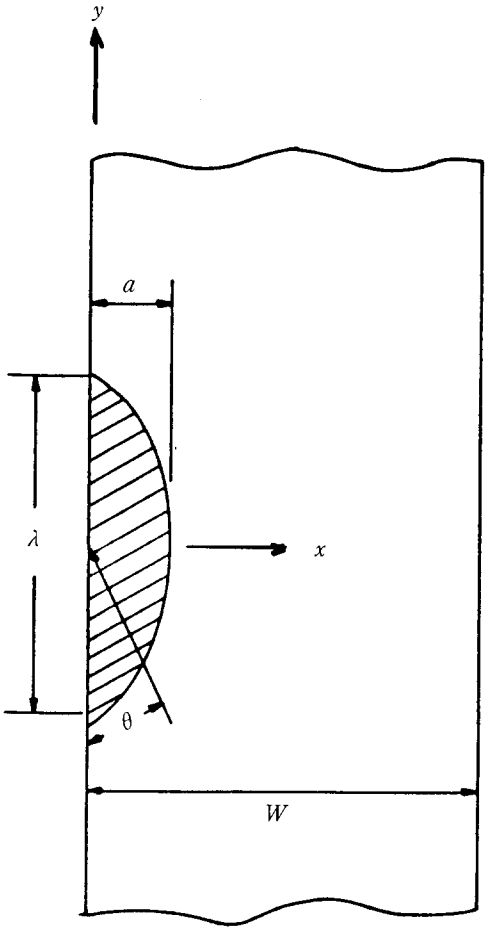

Fig. 2 Semi-elliptical surface crack in an infinite strip

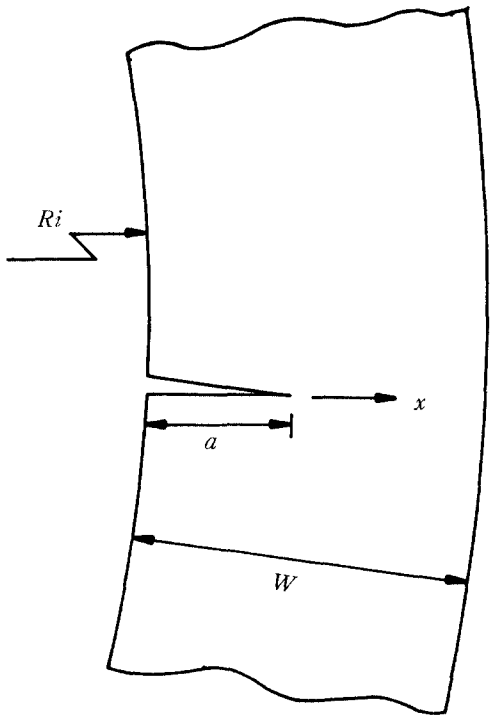

Fig. 3 Continous surface crack in a cylinder

constraint factors such as a semi-elliptical crack shape and a finite crack length.

The weight function is related to the crack shape and crack tip displacement. Crack tip displacement in the cylindrical structure would be more restricted than in the plate. The displacement at an arbitrary x from inner surface (Fig. 3) is a function of the ratio of distance from cylinder center to the crack tip (Rabbens, et. al., 1976). According to Labbens and Heliot (1976), the modified weight function for cylindrical structures could be given as :

$$M(x,\ a)=\left(\frac{R_i+x}{R_i+a}\right)\left(\frac{1}{2\pi(a-x)}\right)^{\frac{1}{2}}\cdot \left[1+m_1\left(\frac{a-x}{a}\right)+m_2\left(\frac{a-x}{a}\right)^2\right] \quad (3)$$

where R_i is an inner radius of cylinder.

1) Consideration of semi-elliptical crack shape

When reviewing the stress intensity factor for semi-elliptical cracked structure, the line integral Φ has been designated a shape factor because its value depends on the aspect ratio (a/λ). Therefore, in this study the line integral was classified as one of the constraint factors. Then the modified stress intensity factor is given as :

$$K_I(a)=\frac{1}{\Phi}\int_0^a \sigma(x)M(x,\ a)dx$$

$$M(x,\ a)=\left(\frac{R_i+x}{R_i+a}\right)\left(\frac{1}{2\pi(a-x)}\right)^{\frac{1}{2}}\cdot \left[1+m_1\left(\frac{a-x}{a}\right)+m_2\left(\frac{a-x}{a}\right)^2\right]$$

$$\Phi=\int_0^{\pi/2}\left[1-\left(\frac{\lambda^2-a^2}{\lambda^2}\right)\sin^2\theta\right]^{\frac{1}{2}}d\theta \quad (4)$$

2) Consideration of finite crack length

According to Eq. (1) the value of weight function at the free surface is $1+m_1+m_2$ and becomes infinite at the crack tip. Furthermore the value of weight function for semi-elliptical cracks with finite crack is much less than that for continuous cracks at any given points between the surface and the crack tip. And, the increasing rate of weight function for semi-elliptical crack to the continuous crack is asymptotically limited. So, with the consideration of best fitting of slower increasing rate for semi-elliptical cracks and assumption that the sinusoidal line integral is the most appropriate correction factor in this case, m_1 and m_2 suggested by Bueckner (1970) is modified as follows :

$$m_1=N_1+O_1\left(\frac{1}{C\Phi^2}\right)\left(\frac{a}{w}\right)^2+P_1\left(\frac{1}{C\Phi^2}\right)\left(\frac{a}{w}\right)^6$$

$$m_2=N_2+O_2\left(\frac{1}{C\Phi^2}\right)\left(\frac{a}{w}\right)^2+P_2\left(\frac{1}{C\Phi^2}\right)\left(\frac{a}{w}\right)^6$$

where C is a constant.

If a/λ is zero, the constant terms represent the values for continuous crack, and if a/λ is one, these constants represent the values for the semi-circular crack.

The stress intensity factor modified by including these geometrical constraint factor is given as :

$$K_I(a)=\frac{1}{\Phi}\int_0^a \sigma(x)M(x,\ a)dx$$

$$M(x,\ a)=\left(\frac{R_i+x}{R_i+a}\right)\left(\frac{1}{2\pi(a-x)}\right)^{\frac{1}{2}}\cdot$$

$$\left[1+m_1\left(\frac{a-x}{a}\right)+m_2\left(\frac{a-x}{a}\right)^2\right]$$

$$m_1=N_1+O_1\left(\frac{1}{C\Phi^2}\right)\left(\frac{a}{w}\right)^2+P_1\left(\frac{1}{C\Phi^2}\right)\left(\frac{a}{w}\right)^6$$

$$m_2=N_2+O_2\left(\frac{1}{C\Phi^2}\right)\left(\frac{a}{w}\right)^2+P_2\left(\frac{1}{C\Phi^2}\right)\left(\frac{a}{w}\right)^6 \quad (5)$$

The arbitrary distributed stress can be expressed by a series of polynomial. However this stress distribution can be fitted by a third degree of polynomial, i. e.,

$$\sigma(x)=A_0+A_1x+A_2x^2+A_3x^3 \quad (6)$$

With inserting the above stress distribution, Eq. (5) becomes :

$$K_I(a)=\frac{1}{\Phi}\int_0^a\left[\left(\frac{R_i+x}{R_i+a}\right)(A_0+A_1x+A_2x^2+A_3x^3)\left(\frac{1}{2\pi(a-x)}\right)^{\frac{1}{2}}\left(1+m_1\left(\frac{a-x}{a}\right)+m_2\left(\frac{a-x}{a}\right)^2\right)\right]dx \quad (7)$$

$$K_I(a)=\frac{1}{\Phi}\left(\frac{a}{2\pi}\right)^{\frac{1}{2}}[A_0(R_if_{01}+af_{02})+A_1(R_if_{11}+2af_{12})a+A_2(R_i2f_{21}+6af_{22})a^2+A_3(R_i6f_{31}+24af_{32})a^3] \quad (8)$$

where

$$f_{01}=2+\frac{2}{3}m_1+\frac{2}{5}m_2$$

$$f_{02}=\frac{4}{3}+\frac{4}{15}m_1+\frac{4}{35}m_2$$

$$f_{11}=f_{02}$$

$$f_{12}=\frac{8}{15}+\frac{8}{45}m_1+\frac{8}{315}m_2$$

$$f_{21}=f_{12}$$

$$f_{22}=\frac{16}{105}+\frac{16}{945}m_1+\frac{16}{3465}m_2$$

$$f_{31}=f_{22}$$

$$f_{32}=\frac{32}{945}+\frac{32}{10395}m_1+\frac{32}{45045}m_2$$

2.1.2 Plasticity deformation failure assessment diagram

If a material's behavior can be represented by deformation plasticity theory and its true stress-true strain relationship by a Ramberg-Osgood power law, such as

$$\frac{\varepsilon}{\varepsilon_o}=\frac{\sigma}{\sigma_o}+\alpha\left(\frac{\sigma}{\sigma_o}\right)^n \quad (9)$$

Simple expressions for the J-integral of the cracked structure can be written as

$$J=J^e(a_{eff}, P)+J^p(a, P, n) \quad (10)$$

where J^e is the elastic contribution based on Irwin's effective crack depth (a_{eff}) and J^p is the deformation plasticity solution. From the handbook (Tada, et. al., 1973), J^e is founded and J^p is provided by EPRI NP-1931 (Rice, 1972) and the stress and strain parameter (σ_o, ε_o) in Eq. (9) can be chosen as the engineering yield strength and yield strain, respectively. α, n are determined by using Eq. (9) and experimental data.

Once Eq. (10) is determined, the deformation plasticity failure assessment curves are defined by dividing the total J-integral of the cracked structure by the elastic J-integral of the structure given by

$$J^e(a, P)=K^2(a, P)\frac{(1-\nu^2)}{E} \quad (11)$$

where K is the linear elastic fracture mechanics stress intensity factor. Eq. (10) becomes

$$\frac{J}{J^e(a, P)}=\frac{1}{K_r^2}=\frac{(J^e(a_{eff}, P)+J^p(a, P, n))}{J^e(a, P)}=f\left(\frac{\sigma}{\sigma_p}\right)=f(S_r) \quad (12)$$

In Eq. (12) K_r represented the ratio of stress intensity factor to fracture toughness and $S_r=\sigma/\sigma_p$ is the applied stress/plastic collapse stress ratio. To use the deformation plasticity failure assessment diagram, assessment points are then plotted on the resulting diagram. The coordinates of these assessment points can be calculated using

$$K_r'=\frac{K}{K_{IC}} \quad (13)$$

$$S_r'=\frac{\sigma}{\sigma_p} \quad (14)$$

where K is the stress intensity factor for the structure and K_{IC} is the fracture toughness of the material. σ is the applied stress on the structure

and σ_p is the plastic collapse stress. For a particular stress level and flaw size, the coordinates (S_r', K_r') can be calculated and if the point lies on or outside of the failure assessment curve, crack growth will initiate. Points inside the curve indicate that the system or structure is safe from the crack initiation. An assessment point is designated by primed symbol, while the failure assessment curve is represented in terms of unprimed S_r and K_r.

Furthermore, Eqs. (13) and (14) can be generalized to include crack initiation

$$K_r'=\sqrt{\frac{J^e(a,\ P)}{J_{IC}}} \tag{15}$$

For stable crack growth (ductile tearing), both K_r' and S_r' must be redefined as

$$K_r'(a_0+\Delta a)=\sqrt{\frac{J^e(a_0+\Delta a)}{J_R(\Delta a)}} \tag{16}$$

$$S_r'(a_0+\Delta a)=\frac{\sigma}{\sigma(a_0+\Delta a)} \tag{17}$$

where J^e, J_R and $\sigma\ (a_o+\Delta a)$ are functions of the amount of slow stable crack growth. J_R is the experimentally measured J-resistance curve plotted as a function of Δa. J^e is calculated as before from the elastic stress intensity factor for the current crack length $(a_o+\Delta a)$.

3. Application Examples

3.1 Stress intensity factor problems

3.1.1 Comparison with other methods

In order to judge the analytically developed expression for the K versus a/λ relationship, the present results were compared to those calculated by Labben et. al. (1976) and pc-CRACK (1989). The parameter used for the comparison is magnification factor.

Labben et. al. (1976) expressed the stress intensity factors as follows:

$$K_I=\sqrt{\pi a}\left[A_0F_1+\frac{2a}{\pi}A_1F_2+\frac{a^2}{2}A_2F_3+\frac{4a^3}{3\pi}A_3F_4\right] \tag{18}$$

where F_1, F_2, F_3, F_4 are magnification factors. Through the use of Eq. (6) to (8), magnification factors for the present method are derived as:

$$F_1=\sqrt{2}[R_if_{01}+af_{02}]\frac{1}{R_i+a}\frac{1}{\pi}$$

$$F_2=\frac{1}{\sqrt{2}}[R_if_{11}+a2f_{12}]\frac{1}{R_i+a}$$

$$F_3=\sqrt{2}[R_i2f_{21}+a6f_{22}]\frac{1}{R_i+a}\frac{1}{\pi}$$

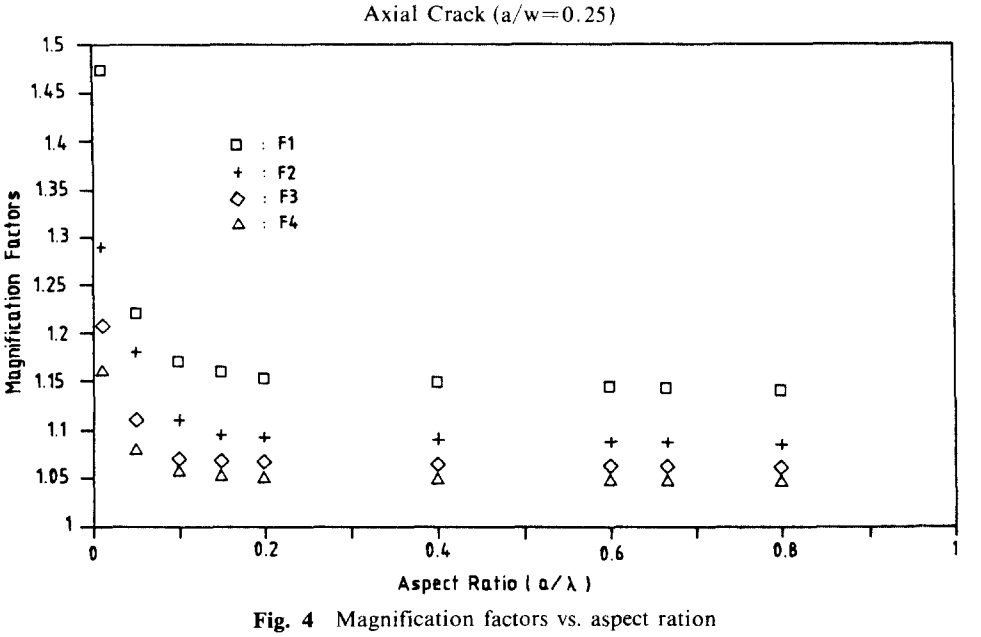

Fig. 4 Magnification factors vs. aspect ration

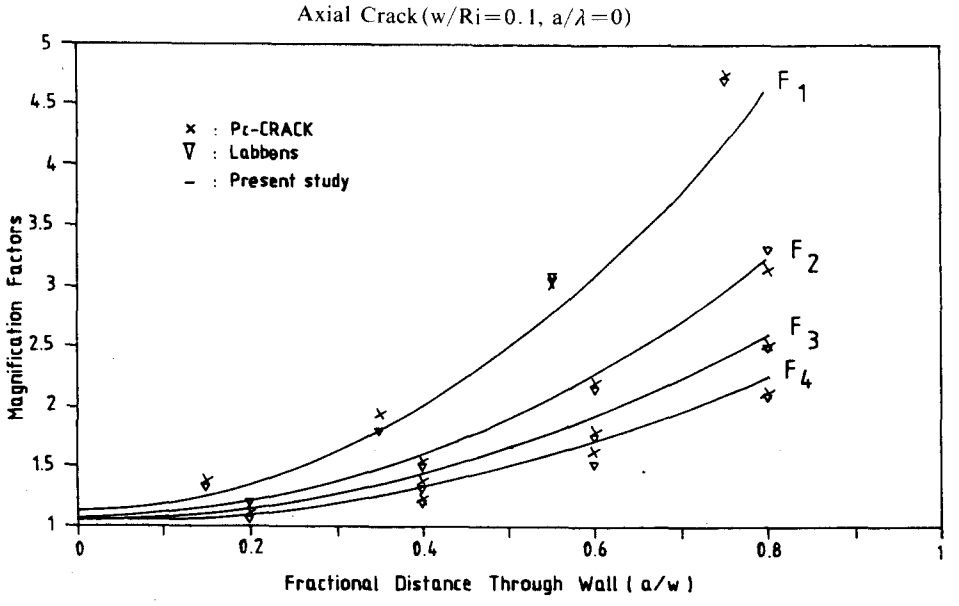

Fig. 5 Magnification factors for continous surface crack in a cylinder

$$F_4=\frac{3}{\sqrt{8}}[R_i 6f_{31}+a24f_{32}]\frac{1}{R_i+a}$$

Figure 4 shows the magnification factors with the variation of crack aspect ratio (a/λ) for $a/w=0.25$. Magnification factors decrease as the crack shape changed from continuous to semi-elliptic. When aspect ratio is above 1.0, magnification factors exhibited almost constant values. The relation between magnification factors and fractional crack depth (a/w) is shown in Fig. 5, including the results of Labbens and pc-CRACK, for the continuous surface crack in cylinder. In Fig. 5, magnification factors calculated by using Eq. (18) are relatively consistent and in good agreement with those from Labbens et. al. (1976) and pc-CRACK (1989).

There are some discrepancies among these values, when a/w is above 0.5. However the use of present method seems reasonable in practical application, since the a/w ratio for real cracks is much smaller than 0.5. It should be noted that constant terms, P_1 and P_2, suggested by Labbens et. al. (1976) were neglected in order to minimize the data deviation and for the best fitting of m_1 and m_2, C is 1. Then, m_1 and m_2 were represented as a second order polynomial terms.

3.1.2 Sample problems

The example is typical of nuclear pressure vessel (Outer Radius : $R=100$ in. (25.4 cm), $w/R=0.1$). Two stress distributions are chosen, which were used in Kim and Sohn (1989), i. e..

$$\sigma_1(x)=40-8.912x+0.974x^2-0.0382x^3 \text{ ksi}$$
$$\sigma_2(x)=40-17.824x+1.946x^2-0.0765x^3 \text{ ksi}$$

(1) Continuous surface crack in cylinder $(a/w=0.25,\ a/\lambda=0)$

Stress intensity factors obtained in this study were compared to the 'pc-CRACK' (1989), as tabulated in Table 1.

The value of stress intensity factor obtained from the present study is obviously closer to FEM values than that of other calculation methods.

(2) Semi-elliptical surface crack in cylinder

Actual cracks in structural elements are often approximated by semi-elliptical cracks. Therefore comparison is extended to ASME-III APP.-G type cracks $(a/\lambda=1/6,\ a/w=0.25)$. The results are shown in Table 2.

The values of the present study is also definitely less conservative than those of other calculation methods (Kim et. al., 1989) and closer to the

Table 1 Stress intensity factors for continuous surface crack

Calculation method	Stress intensity factor (ksi·in.$^{1/2}$)	
	Case of σ_1	Case of σ_2
Maximum stress	174.8	174.8
Linear envelope	154.6	134.3
ASME	129.6	84.3
Present study*	123.5	81.6
FEM by buchalet	115.8	76.4

Table 2 Stress intensity factors for ASME-Ⅲ APP. G-type crack

Calculation method	Stress intensity factor (ksi·in.$^{1/2}$)	
	Case of σ_1	Case of σ_2
Maximum stress	134.7	134.7
Linear envelope	116.9	99.0
ASME	94.8	55.0
Present study*	83.7	52.3
FEM by McGowan	75.8	46.9

FEM values.

3.2 Failure assessment diagram problems

Bloom (1985) used the K expression derived by Newman and Raju (1980) for uniform stress distribution.

To illustrate the use of the weight function in the failure assessment diagram for a beltline crack of $a/t=0.25$, two crack configurations were assumed:

(1) A continuous longitudinal inside surface crack in a pressurized cylinder, $a/\lambda=0.0$;

(2) A semi-elliptical longitudinal inside surface crack in a pressurized cylinder, $a/\lambda=1/6$.

For the comparison of these analyses, Bloom's experimental and analytical data for the uniform stress distribution case were adopted. For the vessel of pressurized to 2.50 ksi (17.24 Mpa) at a temperature of 392°F ($R_i=85$ in. (216 cm), $t=8.5$ in. (21.6 cm)), the J_R resistance curve was given by

$$J_R(\Delta a)=2350(\Delta a)^{0.352} \tag{19}$$

where J_R is in in-lb/in^2 units and Δa is measured in inches.

3.2.1 Realistic stress profile

When the pressure vessel was pressurized as P, the average hoop stress is calculated as follow

$$\sigma=\frac{Pr}{t}$$

But, it was known that the stress inside the vessel surface is the highest and is decreasing along the thickness. Therefore the real stress distribution along the thickness direction was expressed as third order polynomial equation as follow.

$$\sigma(x)=25-5.57x+0.6088x^2 -0.02388x^3,\ \text{ksi} \tag{20}$$

The Ramberg-Osgood stress-strain constants are: $\alpha=3.0$, $n=8.6$, $\sigma_{ys}=85$ ksi (586 MPa). Note that a value of $\delta a=0.010$ in. was used for J_{IC} using the J_R expression given by Eq. (19).

3.3 Failure assessment diagram

To draw the failure assessment diagram curve we used the Bloom's K_r vs S_r relation for $t/R=0.1$, $\nu=0.3$ and expressed

$$\frac{1}{K_r^2}=\frac{a_e}{a}\left(\frac{F(a_e)}{F(a)}\right)^2 +\frac{0.0026(1-a/t)ah_1'S_r^{(n-1)}}{\left[\frac{F(a)}{10\sqrt{Q}}\frac{1-a^*/t}{1+0.1a^*/t}\right]^2}$$

where

$$\frac{a_e}{a}=1+22.22\left(\frac{n-1}{n+1}\right)\cdot \left[\frac{F(a)}{10\sqrt{Q}}\frac{(1-a^*/t)}{(1+0.1a^*/t)}\right]^2\frac{S_R^2}{1-S_r^2}$$

and

$$\frac{F(a_e)}{F(a)}=\frac{[M_1+M_2(a_e/t)^2+M_3(a_e/t)^4]}{[M_1+M_2(a/t)^2+M_3(a/t)^4]} \frac{[1.1524-0.05\sqrt{a_e/t}]}{[1.1524-0.05\sqrt{a/t}]}$$

$h_1'=h_1'(a/t,a/l,t/R,\ n)$

$=6.9$ for *the semi-elliptical crack*

$=7.38$ for *the continuous crack by Bloom*

Table 3 Numerical results for longitudinal continuous crack

Δa in.	J_R in.lb/in^2	S_r'	K_r' Bloom/present	Safety factor bloom/present
0.01	465	0.349	0.909/0.661	1.071/1.157
0.05	818	0.351	0.670/0.467	1.361/1.424
0.1	1045	0.354	0.630/0.421	1.49 /1.577
0.2	1334	0.360	0.480/0.386	1.59 /1.676
0.4	1702	0.373	0.560/0.367	1.63 /1.703
0.6	1962	0.387	0.566/0.367	1.60 /1.649
0.8	2173	0.402	0.582/0.373	1/55 /1.597

Table 4 Numerical results for longitudinal semi-elliptical crack

Δa in.	J_R in.lb/in^2	S_r'	K_r' Bloom/present	Safety factor bloom/present
0.01	465	0.349	0.611/0.449	1.60/2.103
0.05	818	0.351	0.465/0.340	2.03/2.504
0.1	1045	0.354	0.418/0.302	2.20/2.647
0.2	1334	0.360	0.380/0.270	2.33/2.761
0.4	1702	0.373	0.354/0.243	2.40/2.847
0.6	1962	0.387	0.346/0.229	2.39/2.838
0.8	2173	0.402	0.345/0.220	2.35/2.816

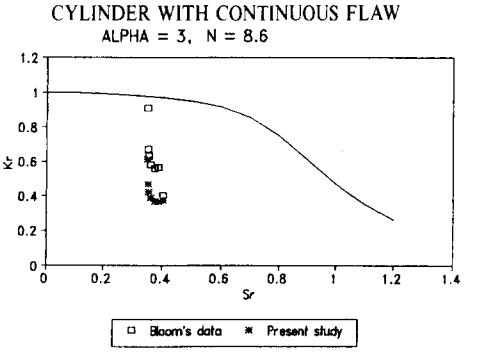

Fig. 6 FAD for cylinder with continous flaw

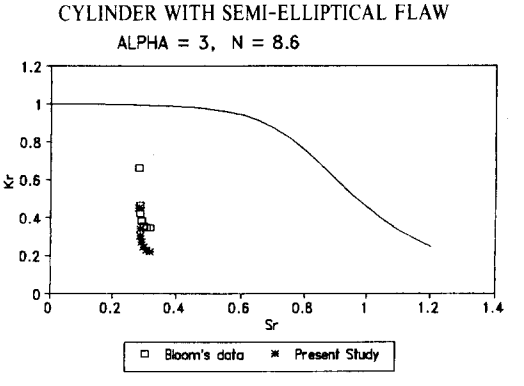

Fig. 7 FAD for cylinder with semi-elliptical flaw

To include semi-elliptical cracks for the J^p fully plastic expression, a was replaced by a^* which was suggested by Central Electricity Generating Board

$$a^*=\frac{a\sqrt{[1-1(1+l^2/2t^2)]}}{\sqrt{[1-a/t(1+l^2/2t^2)]}}$$

For the calculation of failure assessment point, instead of Newman and Raju's K (1980), Eq. (20) was used as K' value. Through Eq. (13) to (17) K_r' and S_r' were calculated and tabulated for the comparison to the existing values.

Figures 6 and 7 illustrates our results and Bloom's. The crack assessment in these examples resulted in the more increased safety margin than that of bloom's stress condition.

For the calculation of the safety factor, make a straight line from the origin to the solid reference curve. The straight line must pass through the corresponding point which represents the K_r, S_r values. The safety factor is defined as the ratio of the reference radial distance with respect to the corresponding radial distance from origin.

In Tables 1, 2 and Figs. 6, 7 a=0.01 in. and 0.04 in. are for the J_{IC} and maximum safety factor, respectively. With the assumption of uniform stress distribution safety factors for crack initiation and maximum safety factor are 1.07 and 1.63, respectively. For the case of realistic stress distribution these safety factors form 1.60 and 2.10 to 2.40 and 2.80.

4. Conclusions

The semi-elliptical crack problems are important especially in the design and fracture analysis of pressure vessels and castings. The complicated 3-dimensional analysis is required in order to obtain the exact solution of stress intensity factors for the semi-elliptical crack problems. However, this complication could be overcome through 2-dimensional approach based on the continuous

crack solution, by taking into account geometric crack characters such as semi-elliptical crack shape and finite crack length. It would be a great advantage and was an objective herein to be able to estimate the K versus a/λ relationship for a semi-elliptical crack. Furthermore, the present stress intensity factor solutions appear less conservative than that of ASME-XI technique and close to the FEM values.

Flaw assessments were performed by the application of DPFAD (Failure Assessment Diagram) approach with the K_I calculation for the realistic stress profile through weight function technique. The remarkable advantage of the weight function is the realistic calculation of the stress intensity factor, which is used for the assessment points in the DPFAD. These approach for failure assessment could lead to prevent the unnecessarily early shutdown of some nuclear power plants, which might be assessed by conservative DPFAD analysis with the assumption of uniform stress distribution.

References

ASME Boiler and Pressure Vessel Code, Section Ⅲ, Appendix G, The American Society of Mechanical Engineers, New York, 1989.

Bueckner, H. F., 1970, "A Novel Principle for the Computation of Stress Intensity Factors," *Z. Angewandte Mathemat, Mechan*, Vol. 50, No. 9, pp. 529~546.

Bloom, J. M., 1983, "Procedure for the Assessment of Structural Integrity of Nuclear Pressure Vessels," *ASME Journal of Pressure Vessel Technoogy*, Vol. 105.

Bloom, J. M., 1985, "Extensions of the Failure Assessment Diagram Approach Semi-Elliptical Flaw in Pressurized Cylinder," *ASME Journal of Pressure Vessel Technology*, Vol. 107.

Bloom, J. M. and Malik, S. N., 1982, "A Procedure for the Assessment of Nuclear Pressure Vessels and Piπng Contaning Defects," EPRI Topical Report NP-2431, Research Project 1237-2, Palo Alto, Calif.

Harrison, R. P., Loosemore, K. and Milne, I., 1976, "Assessment of the Integrity of Structures Containing Defects," CEGB Report No. R/H/6, Central Electricity Generating Board, United Kingdom.

Kim, Y. and Sohn, G. H., 1989, "Engineering Procedures for Determining Stress Intensity Factors for Nonlinear Stress Fields in Pressure Vessel Wall," *Proc. Int. Symp.* on PVNC, Seoul.

Labbens, R., Pessissier-Tanon, A. and Heliot, J., 1976, "Practical Method for Calculating Stress Intensity Factors Through Weight Functions," *ASTM AST-590*, pp. 368~384.

Newman, J. C. and Raju, I. S., 1980, "Stress-Intensity Factors for Internal Surface Cracks in Cylinder Pressure Vessels," *ASME Journal of Pressure Vessel Technology*, Vol. 102.

"pc-CRACK User's Manual," Ver. 2.0, 1989, Structural Integrity Associates.

Rice, J. R., 1972, "Some Remarks on Elastic Crack-Tip Stress Fields," *Int. J. Solids Structures*, No. 6, pp. 751~758.

Rolfe, S. T. and Barson, J. M., 1977, "Fracture and Fatigue Control in Structues-Application of Fracture Mechanics," Prentice-Hall, pp. 34~40.

Tada, H., Paris, P. C. and Irwin, C. G., 1973, "The Stress Analysis of Crack Handbook," Del Research Corporation.